Substructure Model Updating with Noisy Measurements through a Regularized Modal Dynamic Residual Approach

Xinjun Dong, Dapeng Zhu, Yang Wang
Georgia Institute of Technology, Atlanta, GA 30332, USA

Abstract
In order to reduce the discrepancy between an as-built structure and its preliminary finite element (FE) model, selected FE model parameters can be updated based on the experimental data collected from the actual structure. This process is termed as FE model updating. During the past few decades, many FE model updating approaches have been developed. Most of the approaches operate on the entire stucture model, attempting to simultaneously update parameters at difference parts of the structure. When applied to large and complex structures, such approaches suffer computational challenges and convergence issues. To overcome these difficulties, this paper adopts a substructure model updating approach that utilizes the Craig-Bampton transform to reduce model size. Furthermore, this paper also studies the robustness of the substructure model updating approach with noisy measurements that may negatively influence the model updating accuracy. A regularized modal dynamic residual approach is proposed for the substructure model updating with noisy measurments. To evaluate the performance of the substructure model updating approach, Monte Carlo simulation is performed to generate noise-contaminated modal properties of a 200-degree-of-freedom spring mass model. The updating performance is compared with a conventional updating procedure that minimizes analytical and experimental modal property differences.

1. Introduction

Over the past few decades, tremendous progress has been made in finite element (FE) modeling of civil structures. Nevertheless, discrepancies usually exist in structural behavior between the prediction from FE models (built according to design drawings) and actual structures in the field. For example, nominal material properties are usually adopted in FE models, while actual material properties can be different. In another example, idealized connections and support conditions are typically used in structural analysis and design, while these conditions do not exist in reality. As a result, a preliminary FE model may not accurately describe the behavior of the actual structure. To achieve higher accuracy, FE model updating can be performed based on sensor measurements from the actual structure in the field.

Numerous FE model updating methods have been developed in the past few years (Friswell & Mottershead, 1995). The discrepancies between experimental measurement and FE model can be adopted as the minimization objective for FE model updating. Such discrepancy objective can be based on time histories (Hoshiya & Saito, 1984), vibration modes (Jaishi & Ren, 2006), frequency response function (Sipple & Sanayei, 2014), among others. However, most of the existing methods operate on the entire structure model, attempting to simultaneously update parameters at difference parts of the structure. Thus, the methods usually suffer computational challenges and convergence problem when applied on complex structures with a large number of degrees of freedom (DOFs). In order to address the difficulties, some research activities have been devoted to substructure model updating, which focuses on updating one part of a large structure (instead of the entire structure) at a time. For instance, operating in time domain, the extended Kalman filter is applied for substructure model updating of a shear-frame structure (Koh *et al.*, 1991). In other studies, frequency spectra are adopted for substructure identification, by minimizing the difference between simulated and experimental acceleration spectra in certain frequency band (Zhang & Johnson,

2013). In addition, Zhu *et al.* (2014) adopt the Craig-Bampton transform to condense the rest of the structure, and update a substructure by minimizing the modal dynamic residuals from the eigenvalue equations in structural dynamics.

Besides the challenge caused by the scale of large structure models, experimental data is inevitably contaminated with random and systematic measurement noises. The noisy data produces uncertainties in model updating results, which negatively influence FE model updating accuracy. Researchers have investigated noise effect reduction for some FE model updating approaches. For example, some researchers adopted Bayesian estimation in model updating to reduce the influence of measurement noises (Alvin, 1997; Collins *et al.*, 1974). In addition, Ahmadian *et al.* (1998) investigated the regularization of model parameter change in the objective function for FE model updating using noisy measurements. The application of truncated singular value decomposition (SVD) approach is also studied by Park *et al.* (2007).

This research studies substructure model updating using noise-contaminated vibration modal properties. Following the approach proposed by Zhu *et al.* (2014), the residual structure is condensed through the Craig-Bampton transform. A regularized modal dynamic residual approach is proposed as the optimization problem for model updating. An iterative linearization procedure is adopted for efficiently solving the optimization problem (Farhat & Hemez, 1993). To evaluate the reliability of the substructure model updating approach, Monte Carlo simulation is performed to generate noise-contaminated modal properties of a 200-DOF spring mass model. The rest of the paper is organized as follows. Section 2 presented the formulation of substructure modeling and model updating through the regularized modal dynamic residual approach. Section 3 described Monte Carlo simulation on a 200-DOF spring-mass model. The performance of the proposed model updating approach is compared with a conventional updating procedure that minimizes experimental and simulated modal property differences. Finally, Section 4 provides a summary and discussion.

2. Formulation for Substrucutre Modeling and Updating

This section presents the basic formulation for substructure updating. Section 2.1 describes substructure modeling strategy following the Craig-Bampton transform. Section 2.2 describes substructure model updating through the regularized modal dynamic residual approach.

2.1. Substructure Modeling

Figure 1 illustrates the substructure modeling strategy. The substructure being analyzed, the interface nodes, and the residual structure are denoted by subscripts S, I, and R, respectively. The block tri-diagonal structural stiffness and mass matrices, $\mathbf{K}$ and $\mathbf{M}$, can be assembled using original degrees of freedom (DOFs): $\mathbf{x} = [\mathbf{x}_S \quad \mathbf{x}_I \quad \mathbf{x}_R]^T$.

$$\mathbf{K} = \begin{bmatrix} \begin{bmatrix} \mathbf{K}_S \end{bmatrix} & \mathbf{0} \\ \mathbf{0} \quad \mathbf{0} & \mathbf{0} \end{bmatrix} + \begin{bmatrix} \mathbf{0} & \mathbf{0} \quad \mathbf{0} \\ \mathbf{0} & \begin{bmatrix} \mathbf{K}_R \end{bmatrix} \end{bmatrix} = \begin{bmatrix} \begin{bmatrix} \mathbf{K}_{SS} & \mathbf{K}_{SI} \\ \mathbf{K}_{IS} & \mathbf{K}_{II}^S \end{bmatrix} & \mathbf{0} \\ \mathbf{0} \quad \mathbf{0} & \mathbf{0} \end{bmatrix} + \begin{bmatrix} \mathbf{0} & \mathbf{0} \quad \mathbf{0} \\ \mathbf{0} & \begin{bmatrix} \mathbf{K}_{II}^R & \mathbf{K}_{IR} \\ \mathbf{K}_{RI} & \mathbf{K}_{RR} \end{bmatrix} \end{bmatrix} \tag{1}$$

$$\mathbf{M} = \begin{bmatrix} \begin{bmatrix} \mathbf{M}_S \end{bmatrix} & \mathbf{0} \\ \mathbf{0} \quad \mathbf{0} & \mathbf{0} \end{bmatrix} + \begin{bmatrix} \mathbf{0} & \mathbf{0} \quad \mathbf{0} \\ \mathbf{0} & \begin{bmatrix} \mathbf{M}_R \end{bmatrix} \end{bmatrix} = \begin{bmatrix} \begin{bmatrix} \mathbf{M}_{SS} & \mathbf{M}_{SI} \\ \mathbf{M}_{IS} & \mathbf{M}_{II}^S \end{bmatrix} & \mathbf{0} \\ \mathbf{0} \quad \mathbf{0} & \mathbf{0} \end{bmatrix} + \begin{bmatrix} \mathbf{0} & \mathbf{0} \quad \mathbf{0} \\ \mathbf{0} & \begin{bmatrix} \mathbf{M}_{II}^R & \mathbf{M}_{IR} \\ \mathbf{M}_{RI} & \mathbf{M}_{RR} \end{bmatrix} \end{bmatrix} \tag{2}$$

Here $\mathbf{K}_S$ and $\mathbf{M}_S$ are the stiffness and mass matrices corresponding to the substructure; $\mathbf{K}_R$ and $\mathbf{M}_R$ denote the residual structure entries; $\mathbf{K}_{II}^S$ and $\mathbf{M}_{II}^S$ denote the entries at the interface DOFs

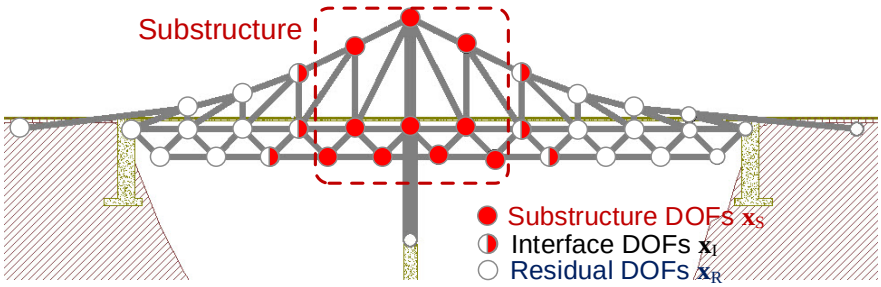

Figure 1. Illustration of substructure modeling strategy

and contributed by the substructure; $\mathbf{K}_{II}^{R}$ and $\mathbf{M}_{II}^{R}$ denote entries at the interface DOFs and contributed by the residual structure.

The dynamic behavior of the residual structure can be approximated using the Craig-Bampton transform (Craig & Bampton, 1968). The DOFs of the residual structure, $\mathbf{x}_R \in \mathbb{R}^{n_R}$, are approximated by a linear combination of interface DOFs, $\mathbf{x}_I \in \mathbb{R}^{n_I}$, and modal coordinates of the residual structure, $\mathbf{q}_R \in \mathbb{R}^{n_q}$.

$$\mathbf{x}_R \approx \mathbf{T}\mathbf{x}_I + \mathbf{\Phi}_R \mathbf{q}_R \tag{3}$$

Here $\mathbf{T} = \left[-\mathbf{K}_{RR}^{-1}\mathbf{K}_{RI}\right] \in \mathbb{R}^{n_R \times n_I}$, is the Guyan static condensation matrix; $\mathbf{\Phi}_R = \left[\phi_1, \cdots, \phi_{n_q}\right] \in \mathbb{R}^{n_R \times n_q}$ represents the mode shapes of the residual structure with interface DOFs fixed. Although the size of the residual structure may be large, the number of modal coordinates, n_q, can be selected as relatively small to only reflect the first few dominant mode (i.e. $n_q << n_R$). The coordinate transformation can be written in vector form as:

$$\begin{bmatrix} \mathbf{x}_I \\ \mathbf{x}_R \end{bmatrix} \approx \mathbf{\Gamma} \begin{bmatrix} \mathbf{x}_I \\ \mathbf{q}_R \end{bmatrix}, \text{ where } \mathbf{\Gamma} = \begin{bmatrix} \mathbf{I} & \\ \mathbf{T} & \mathbf{\Phi}_R \end{bmatrix} \tag{4}$$

The transformation effectively condenses matrices of the residual structure, from $\mathbf{K}_R$ and $\mathbf{M}_R \in \mathbb{R}^{(n_I+n_R)\times(n_I+n_R)}$ to $\widetilde{\mathbf{K}}_R$ and $\widetilde{\mathbf{M}}_R \in \mathbb{R}^{(n_I+n_q)\times(n_I+n_q)}$, respectively (Zhu *et al.*, 2014). Link (1998) described a model updating method for both the substructure and the residual structure. The substructure model is updated as:

$$\mathbf{K}_S = \mathbf{K}_{S0} + \sum_{j=1}^{n_\alpha} \alpha_j \mathbf{K}_{S0,j} \tag{5a}$$

$$\mathbf{M}_S = \mathbf{M}_{S0} + \sum_{j=1}^{n_\beta} \beta_j \mathbf{M}_{S0,j} \tag{5b}$$

where $\mathbf{K}_{S0}$ and $\mathbf{M}_{S0}$ are the stiffness and mass matrices of the substructure and used as initial starting point in the model updating; α_j and β_j correspond to physical system parameters to be updated, such as elastic modulus and density of each substructure element; n_α and n_β represent the total number of corresponding parameters to be updated; $\mathbf{K}_{S0,j}$ and $\mathbf{M}_{S0,j}$ are constant matrices determined by the type and location of these parameters. Subscript "0" will be used hereinafter to denote variables associated with the initial structural model, which serves as the starting point for model updating. Similarly, the residual structure model is updated as:

$$\tilde{\mathbf{K}}_{\mathrm{R}} = \tilde{\mathbf{K}}_{\mathrm{R0}} + \sum_{j=1}^{n_{\mathrm{I}}+n_q} \zeta_j \tilde{\mathbf{K}}_{\mathrm{R0},j} \tag{6a}$$

$$\tilde{\mathbf{M}}_{\mathrm{R}} = \tilde{\mathbf{M}}_{\mathrm{R0}} + \sum_{j=1}^{n_{\mathrm{I}}+n_q} \eta_j \tilde{\mathbf{M}}_{\mathrm{R0},j} \tag{6b}$$

where ζ_j and η_j are the modal parameters to be updated; $\tilde{\mathbf{K}}_{\mathrm{R0}}$ and $\tilde{\mathbf{M}}_{\mathrm{R0}}$ are the initial stiffness and mass matrices of the condensed residual structure model. Detailed formulations can be found in Zhu *et al.* (2014). $\tilde{\mathbf{K}}_{\mathrm{R0},j}$ and $\tilde{\mathbf{M}}_{\mathrm{R0},j}$ represent the constant correction matrices formulated using modal back-transform.

Using matrix formulations in Eq. (5) for substructure and Eq. (6) for residual structure, the condensed structural model with reduced DOFs, $[\mathbf{x}_{\mathrm{S}} \quad \mathbf{x}_{\mathrm{I}} \quad \mathbf{q}_{\mathrm{R}}]^{\mathrm{T}}$, can be updated with variables α_j, β_j, ζ_j and η_j. For brevity, these variables will be referred to in vector form as $\boldsymbol{\alpha} \in \mathbb{R}^{n_\alpha}$, $\boldsymbol{\beta} \in \mathbb{R}^{n_\beta}$, $\boldsymbol{\zeta} \in \mathbb{R}^{n_{\mathrm{I}}+n_q}$ and $\boldsymbol{\eta} \in \mathbb{R}^{n_{\mathrm{I}}+n_q}$. For example, the condensed stiffness matrix for the entire structure can be written as:

$$\begin{aligned}
\tilde{\mathbf{K}} &= \begin{bmatrix} \begin{bmatrix} \mathbf{K}_{\mathrm{S}} \end{bmatrix} & \mathbf{0} \\ \mathbf{0} \quad \mathbf{0} & \mathbf{0} \end{bmatrix} + \begin{bmatrix} \mathbf{0} & \mathbf{0} & \mathbf{0} \\ \mathbf{0} & \begin{bmatrix} \tilde{\mathbf{K}}_{\mathrm{R}} \end{bmatrix} \\ \mathbf{0} & \end{bmatrix} \\
&= \tilde{\mathbf{K}}_0 + \sum_{j=1}^{n_\alpha} \alpha_j \begin{bmatrix} \begin{bmatrix} \mathbf{K}_{\mathrm{S0},j} \end{bmatrix} & \mathbf{0} \\ \mathbf{0} \quad \mathbf{0} & \mathbf{0} \end{bmatrix} + \sum_{j=1}^{n_{\mathrm{I}}+n_q} \zeta_j \begin{bmatrix} \mathbf{0} & \mathbf{0} & \mathbf{0} \\ \mathbf{0} & \begin{bmatrix} \tilde{\mathbf{K}}_{\mathrm{R0},j} \end{bmatrix} \\ \mathbf{0} & \end{bmatrix} \\
&= \tilde{\mathbf{K}}_0 + \sum_{j=1}^{n_\alpha} \alpha_j \mathbf{S}_{\alpha,j} + \sum_{j=1}^{n_{\mathrm{I}}+n_q} \zeta_j \mathbf{S}_{\zeta,j}
\end{aligned} \tag{7}$$

by defining

$$\tilde{\mathbf{K}}_0 = \begin{bmatrix} \begin{bmatrix} \mathbf{K}_{\mathrm{S0}} \end{bmatrix} & \mathbf{0} \\ \mathbf{0} \quad \mathbf{0} & \mathbf{0} \end{bmatrix} + \begin{bmatrix} \mathbf{0} & \mathbf{0} & \mathbf{0} \\ \mathbf{0} & \begin{bmatrix} \tilde{\mathbf{K}}_{\mathrm{R0}} \end{bmatrix} \\ \mathbf{0} & \end{bmatrix} \tag{8}$$

Similarly, the condensed mass matrix for the entire structure is written as:

$$\tilde{\mathbf{M}} = \tilde{\mathbf{M}}_0 + \sum_{j=1}^{n_\beta} \beta_j \begin{bmatrix} \begin{bmatrix} \mathbf{M}_{\mathrm{S0},j} \end{bmatrix} & \mathbf{0} \\ \mathbf{0} \quad \mathbf{0} & \mathbf{0} \end{bmatrix} + \sum_{j=1}^{n_{\mathrm{I}}+n_q} \eta_j \begin{bmatrix} \mathbf{0} & \mathbf{0} & \mathbf{0} \\ \mathbf{0} & \begin{bmatrix} \tilde{\mathbf{M}}_{\mathrm{R0},j} \end{bmatrix} \\ \mathbf{0} & \end{bmatrix} = \tilde{\mathbf{M}}_0 + \sum_{j=1}^{n_\beta} \beta_j \mathbf{S}_{\beta,j} + \sum_{j=1}^{n_{\mathrm{I}}+n_q} \eta_j \mathbf{S}_{\eta,j} \tag{9}$$

where $\mathbf{S}_{\alpha,j}$, $\mathbf{S}_{\beta,j}$, $\mathbf{S}_{\zeta,j}$ and $\mathbf{S}_{\eta,j}$ represent the constant sensitivity matrices corresponding to variables α_j, β_j, ζ_j and η_j, respectively.

2.2. Substructure model updating through the regularized modal dynamic residual approach

To update the substructure model, a regularized modal dynamic residual approach is presented in this study. The model updating approach aims to minimize the summation of modal dynamic residual of the generalized eigenvalue equation and a regularization term.

$$\underset{\boldsymbol{\alpha},\boldsymbol{\beta},\boldsymbol{\zeta},\boldsymbol{\eta},\boldsymbol{\psi}_{\text{unmeas}}}{\text{minimize}} \quad \sum_{j=1}^{n_{\text{meas}}} \left\| \left(\tilde{\mathbf{K}}(\boldsymbol{\alpha},\boldsymbol{\zeta}) - \omega_j^2 \tilde{\mathbf{M}}(\boldsymbol{\beta},\boldsymbol{\eta}) \right) \begin{Bmatrix} \boldsymbol{\psi}_{\text{meas},j} \\ \boldsymbol{\psi}_{\text{unmeas},j} \end{Bmatrix} \right\|^2 + \lambda^2 \left\| \{\boldsymbol{\alpha} \;\; \boldsymbol{\zeta} \;\; \boldsymbol{\beta} \;\; \boldsymbol{\eta}\}^{\text{T}} \right\|^2 \tag{10}$$

where $\|\cdot\|$ denotes any norm function; n_{meas} denotes the number of measured modes from experiments; ω_j denotes the j-th modal frequency extracted from experimental data; $\boldsymbol{\psi}_{\text{meas},j}$ denotes the entries in the j-th mode shape that correspond to measured (instrumented) DOFs; $\boldsymbol{\psi}_{\text{unmeas},j}$ corresponds to unmeasured DOFs; $\boldsymbol{\alpha}$, $\boldsymbol{\beta}$, $\boldsymbol{\zeta}$ and $\boldsymbol{\eta}$ are the selected parameters to be updated (see Eq. (7) and (9)); λ is the regularization parameter, which balances the weightings between modal dynamic residuals and parameter changes from the initial FE model. The regularized objective helps to limit erratic changes in the system updating parameters, particularly when measurement noise is present (Ahmadian *et al.*, 1998). Although the selection of regularization parameter λ deserves in-depth study, in this preliminary research, a constant regularization parameter is adopted.

In summary, the optimization variables are system parameters $\boldsymbol{\alpha}$, $\boldsymbol{\beta}$, $\boldsymbol{\zeta}$, $\boldsymbol{\eta}$ and mode shape entries corresponding to unmeasured DOFs, $\boldsymbol{\psi}_{\text{unmeas},j}$. Eq. (10) leads to a complex nonlinear optimization problem that is generally difficult to solve. However, an iterative linearization procedure for efficiently solving the optimization problem is adopted in this study, similar to (Farhat & Hemez, 1993). Figure 2 shows the pseudo code of the procedure. Each iteration step involves two operations, modal expansion and parameter updating. The operation (i) is modal expansion for unmeasured DOFs, where system parameters ($\boldsymbol{\alpha}$, $\boldsymbol{\beta}$, $\boldsymbol{\zeta}$ and $\boldsymbol{\eta}$) are treated as constant. When model parameters are held constant, $\boldsymbol{\psi}_{\text{unmeas},j}$ (j=1,…, n_{meas}) become the optimization variables in Eq. (10). The operation (ii) at each iteration is the updating of system parameters ($\boldsymbol{\alpha}$, $\boldsymbol{\beta}$, $\boldsymbol{\zeta}$ and $\boldsymbol{\eta}$) using the expanded mode shapes. Thus, $\boldsymbol{\psi}_{\text{unmeas},j}$ (j=1,…, n_{meas}) is held as constant in operation (ii); the system parameters are optimization variables. When 2-norm is used in Eq. (10), the optimization problem in both operations becomes a simple regularized least square problem.

3. Numerical Example

To validate the regularized modal dynamic residual approach for substructure model updating with noisy measurement, simulation is performed on a generic 200-DOF spring-mass model. For the initial model, all the mass and spring stiffness values are set identically as 6 kg and 35kN/m, respectively. 20%, 30%, 40% of spring stiffness increase is introduced to k_{45}, k_{48}, k_{50}, respectively, and 10% of spring stiffness decrease is introduced to k_5, k_{10}, k_{12}, k_{60}, k_{80}, k_{120}, k_{150}. Figure 3 shows a conceptual drawing of the 200-DOF spring-mass numerical model with marked spring stiffness change, as well as substructure, interface and residual DOFs. A substructure including DOFs from 41 to 54 is selected for model updating. DOFs 40 and 55 are the interface DOFs, and all other DOFs belong to the residual structure. Dynamic response of the residual structure is approximated using 20 modal coordinates, i.e. n_q = 20 in Eq. (3). With the substructure DOF vector, $\mathbf{x}_S \in \mathbb{R}^{14\times 1}$ and the

start with $\boldsymbol{\alpha}$, $\boldsymbol{\beta}$, $\boldsymbol{\zeta}$ and $\boldsymbol{\eta}$ = 0 (meaning $\mathbf{M}$ and $\mathbf{K}$ start with initial values at $\mathbf{M}_0$ and $\mathbf{K}_0$) ;

REPEAT {

(i) hold $\boldsymbol{\alpha}$, $\boldsymbol{\beta}$, $\boldsymbol{\zeta}$ and $\boldsymbol{\eta}$ as constant and minimize Eq.(10) over variable $\boldsymbol{\psi}_{\text{unmeas},j}$ (j = 1,…,n_{meas});

(ii) hold $\boldsymbol{\psi}_{\text{unmeas},j}$ (j = 1,…,n_{meas}) as constant and minimize Eq.(10) over variables $\boldsymbol{\alpha}$, $\boldsymbol{\beta}$, $\boldsymbol{\zeta}$ and $\boldsymbol{\eta}$;

} UNTIL convergence ;

Figure 2. Pseudo code of the iterative linearization procedure.

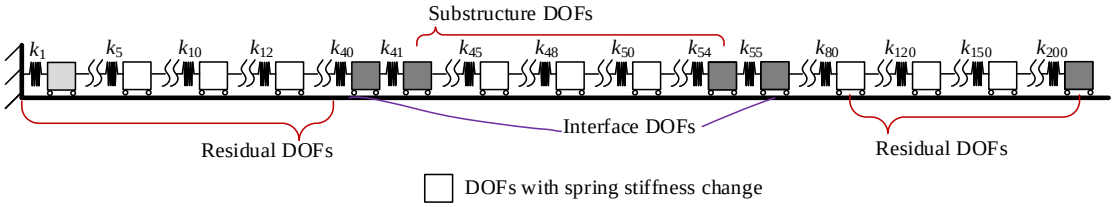

Figure 3. Illustration of damage locations and substructure selection

Table 1. Actual and initial stiffness values for substructure elements (10^4 N/m)

Spring stiffness	k_{41}	k_{42}	k_{43}	k_{43}	k_{44}	k_{45}	k_{46}	k_{47}	k_{48}	k_{49}	k_{50}	k_{51}	k_{52}	k_{53}	k_{54}	k_{55}
Actual value	3.50	3.50	3.50	3.50	3.50	4.20	3.50	3.50	4.55	3.50	4.90	3.50	3.50	3.50	3.50	3.50
Initial value	3.50	3.50	3.50	3.50	3.50	3.50	3.50	3.50	3.50	3.50	3.50	3.50	3.50	3.50	3.50	3.50

interface DOF vector, $\mathbf{x}_I \in \mathbb{R}^{2\times 1}$, the entire structural model is condensed to 36 DOFs (from 200 DOFs in the original structure). Note that three springs with increased stiffness, k_{45}, k_{48}, and k_{50}, are contained in the substructure. Without loss of generality, accurate structural mass matrix is assumed to be known, therefore, mass parameters $\boldsymbol{\beta}$ (Eq. (10)) are not among the updating parameters. Assuming acceleration measurements are available only on the substructure and interface DOFs, the objective is to identify the actual spring stiffness in the substructure. Table 1 lists the actual stiffness values for substructure elements and initial stiffness values for substructure model updating.

For simplicity, the natural frequencies and mode shapes are directly obtained from solving the generalized eigenvalue equation, and used as "experimental" results for model updating. Random errors in normal distribution are assigned to every natural frequency and mode shape vector.

$$\tilde{\boldsymbol{\psi}}_j = \boldsymbol{\psi}_j + \boldsymbol{\varsigma}_j, \quad j = 1,\cdots,n_{\text{meas}} \tag{11}$$

$$\tilde{\omega}_j = \omega_j \cdot \left(1+\xi_j\right), \quad j = 1,\cdots,n_{\text{meas}} \tag{12}$$

where $\boldsymbol{\psi}_j$ denotes the normalized j-th mode shape with maximum entry magnitude equal to 1; $\boldsymbol{\varsigma}_j$ denotes a zero-mean Gaussian random vector; ξ_j denotes the relative random error in normal distribution (zero mean) for the j-th frequency. In this study, a standard deviation of 0.01 is assigned to all entries of $\boldsymbol{\varsigma}_j$ and ξ_j. Note that $\boldsymbol{\varsigma}_j$ and ξ_j are independent.

For comparison, substructure model updating is also performed using a conventional model updating approach. The conventional model updating formulation aims to minimize the difference between experimental and simulated natural frequencies, mode shapes, as well as the unit load surface of the substructure.

$$\underset{\boldsymbol{\alpha},\boldsymbol{\xi},\boldsymbol{\eta}}{\text{minimize}} \quad \sum_{j=1}^{n_{\text{meas}}} w_1^2 \left\{ \left(\frac{\omega_j^{\text{FE}} - \omega_j}{\omega_j} \right)^2 + \left(\frac{1-\sqrt{\text{MAC}_j}}{\sqrt{\text{MAC}_j}} \right)^2 \right\} + w_2^2 \frac{n_{\text{meas}}}{N} \sum_{j=1}^{N} \left(\frac{u_j^{\text{FE}} - u_j}{u_j} \right)^2 \tag{13}$$

Here w_1 and w_2 are constant weighting factors; ω_j^{FE} and ω_j represent the j-th simulated (from the condensed model in Eq. (7) and (9)) and experimentally extracted frequencies, respectively; MAC_j represents the modal assurance criterion evaluating the difference between the j-th simulated and experimental mode shapes. Note that mode shape entries only corresponding to measured DOFs are compared (i.e. between $\boldsymbol{\psi}_{\mathrm{meas},j}^{\mathrm{FE}}$ and $\boldsymbol{\psi}_{\mathrm{meas},j}$); N is total number of DOFs in the condensed system, which equals $n_{\mathrm{S}}+n_{\mathrm{I}}+n_q=$ 36 in this example; u_j^{FE} and u_j represent the j-th entry of analytical and experimental unit load surface (Jaishi & Ren, 2005). The unit load surface vector, $\mathbf{u} \in \mathbb{R}^N$, can be calculated from the modal flexibility matrix $\mathbf{F} \in \mathbb{R}^{N\times N}$ as:

$$\mathbf{u} = \mathbf{F} \cdot \mathbf{l} \tag{14a}$$

$$\mathbf{F} = \begin{bmatrix} \boldsymbol{\psi}_1 & \boldsymbol{\psi}_2 & \cdots & \boldsymbol{\psi}_{n_{\mathrm{meas}}} \end{bmatrix} \begin{bmatrix} 1/\omega_1^2 & 0 & \cdots & 0 \\ 0 & 1/\omega_2^2 & \cdots & 0 \\ \vdots & \vdots & \ddots & \vdots \\ 0 & 0 & \cdots & 1/\omega_{n_{\mathrm{meas}}}^2 \end{bmatrix} \begin{bmatrix} \boldsymbol{\psi}_1^{\mathrm{T}} \\ \boldsymbol{\psi}_2^{\mathrm{T}} \\ \vdots \\ \boldsymbol{\psi}_{n_{\mathrm{meas}}}^{\mathrm{T}} \end{bmatrix} \tag{14b}$$

where $\mathbf{l} \in \mathbb{R}^N$ is a unit load vector with all entries equal to one. Note that when calculating experimental modal flexibility matrix, operation (i)-modal expansion introduced in the modal dynamic residual approach is performed to obtain complete mode shapes. A nonlinear least-square optimization solver, '`lsqnonlin`' in MATLAB toolbox (MathWorks Inc., 2005), is adopted to numerically solve the optimization problem minimizing modal property difference.

Monte Carlo simulation is performed for J = 10,000 runs to generate J sets of "noisy" modal properties. The noisy modal properties are used as experimental data input for model updating. For consistency in comparing the two model updating approaches, at the beginning of each group of 10,000 simulations, the random seed in MATLAB is fixed to generate the same J sets of noisy modal properties for both approaches. The root mean square (RMS) of the relative difference between updated and actual parameters is calculated to evaluate the updating performance for each parameter.

$$\mathrm{RMS}_i = \sqrt{\frac{1}{J}\sum_{j=1}^{J}\left(\frac{\alpha_{i,j}^{\mathrm{upd}} - \alpha_i^{\mathrm{act}}}{\alpha_i^{\mathrm{act}}}\right)^2}, \quad i = 1,\cdots,n_\alpha \tag{15}$$

where α_i^{act} denotes the actual value of the i-th updating parameter (Table 1), and $\alpha_{i,j}^{\mathrm{upd}}$ represents the updated optimal value of the i-th parameter in the j-th run. In this numerical study, the updating parameters α_i simply refer to stiffness parameters k_i.

For reference, both model updating approaches are first applied when no noise is added to experimental modal properties. The initial guesses of the stiffness parameters are all assigned to be 3.5×10^4 N/m, different from actual values (Table 1). Because no noise is present, the regularization parameter λ in Eq. (10) is set to zero; In order to balance the weighing between the difference of natural frequencies and mode shapes, and the difference of unit load surface, weighting factors w_1 and w_2 in Eq. (13) are set to 10 and 1, respectively. For each model updating approach, the updating is performed assuming different numbers of measured modes are available (i.e. modes corresponding to the 2, 3, 4 or 6 lowest natural frequencies). The simulation results show that both

model updating approaches can almost achieve ideal solutions in all scenarios when the data is noise-free. The average RMS error of updating parameters is at the order of 10^{-4}.

Using noisy modal properties generated from Monte Carlo simulation, both model updating approaches are again performed. Regularization parameter λ in Eq. (10) is set to 10,000. With noisy measurement, the modal flexibility component in the modal property difference approach (Eq. (13)) is found to degrade the model updating results, so w_1 and w_2 in Eq. (13) are set to 1 and 0, respectively. Table 2 summarizes the RMS error of each updated stiffness parameter inside the substructure, as well as the average RMS error of each row for the modal dynamic residual approach. As expected, updating results improve as the number of measured modes increases. When the number of available modes increases from 2 to 6, the average error decreases monotonically from 5.12% to 2.43% for the modal dynamic residual approach. Figure 4 shows the histograms of selected updated results (k_{42}, k_{45}, k_{48} and k_{50}) through the modal dynamic residual approach, when different numbers of modes are available. The actual values of the updating parameters (i.e., ideal solution) are represented using vertical lines in each plot. When the number of available modes increases, the variance of the updated parameter decreases, and the bias from actual values also reduces, particularly for k_{42}.

Table 2. RMS error (%) of model updating results using the regularized modal dynamic residual approach

# of modes	k_{41}	k_{42}	k_{43}	k_{44}	k_{45}	k_{46}	k_{47}	k_{48}	k_{49}	k_{50}	k_{51}	k_{52}	k_{53}	k_{54}	k_{55}	Avg. error
2	12.6	8.62	5.66	4.29	2.91	3.42	3.00	2.52	3.36	2.12	3.27	4.75	5.81	6.22	8.18	5.12
3	9.61	7.24	5.04	4.01	2.70	3.33	2.88	2.33	3.24	2.03	3.01	3.83	4.36	4.37	4.40	4.16
4	7.61	6.09	4.46	3.72	2.55	3.19	2.75	2.16	3.05	1.98	2.85	3.20	3.39	3.28	3.24	3.57
6	2.80	2.64	2.64	2.80	2.08	2.40	2.03	1.57	3.03	1.74	2.28	2.55	2.64	2.66	2.60	2.43

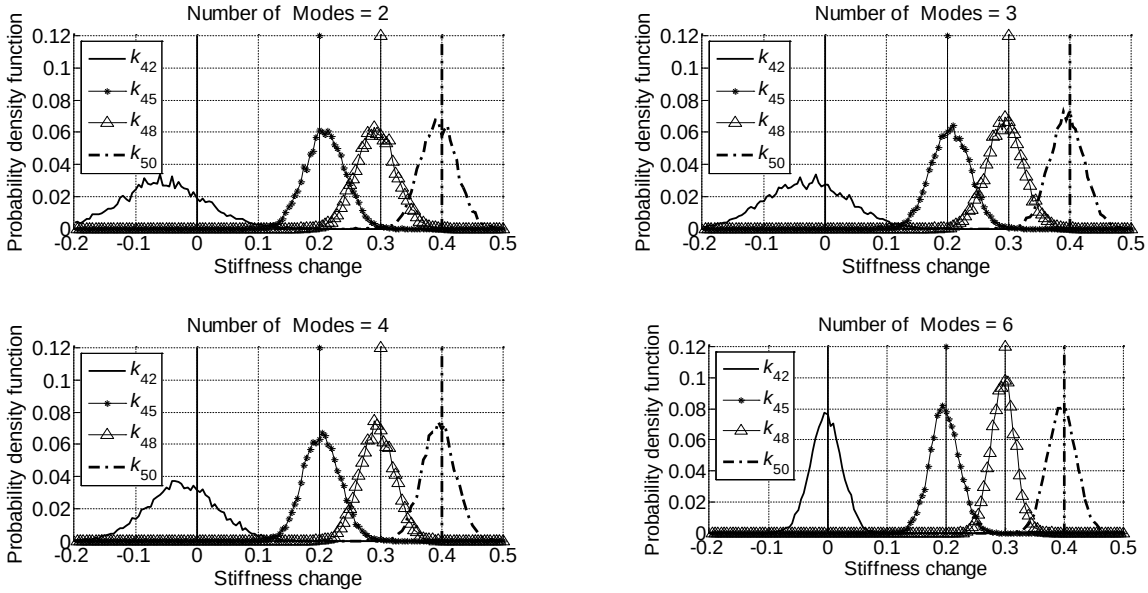

Figure 4. Histogram of selected parameters using the regularized modal dynamic residual approach

Similarly, Table 3 shows the model updating results from the modal property difference approach when 2, 3, 4 and 6 modes are available. It can be seen that in all scenarios, large error happens at DOFs where stiffness change is introduced (k_{45}, k_{48} and k_{50}), and the largest errors are always with k_{50} where the greatest stiffness change is introduced. In the meantime, the average error of the modal dynamic residual approach is lower than that of the modal property difference approach for all scenarios. Figure 5 shows the histogram of selected updated results (k_{42}, k_{45}, k_{48} and k_{50}) through the modal property difference approach when 2, 3, 4 and 6 modes are available. The updated parameters are mainly concentrated at zero, meaning the optimization solver likely stopped at a local minimum near the initial point. It can be demonstrated that in this example, although both modal dynamic residual approach and modal property difference approach can achieve excellent results in noise-free case, the modal dynamic residual approach performs better than modal property difference approach when measurement is contaminated with noise.

4. Conclusion

This research investigates the robustness of a regularized modal dynamic residual approach for substructure model updating against measurement noise. The entire structural model is divided into the substructure (currently being analyzed) and the residual structure. The Craig-Bampton transform is adopted to condense the residual structure. The proposed approach adopted the modal dynamic residual with regularization on model parameters as objective function to update the

Table 3. RMS error (%) of model updating results by modal property difference approach

# of modes	k_{41}	k_{42}	k_{43}	k_{44}	k_{45}	k_{46}	k_{47}	k_{48}	k_{49}	k_{50}	k_{51}	k_{52}	k_{53}	k_{54}	k_{55}	Avg. error
2	15.6	15.1	14.5	14.3	18.4	14.2	14.0	20.7	14.3	25.5	13.4	13.9	14.2	14.7	14.9	15.6
3	3.68	3.98	4.91	6.30	11.2	8.50	9.29	15.8	9.99	21.9	8.62	7.32	6.00	4.77	3.55	8.28
4	1.62	2.18	2.23	1.84	16.2	2.08	2.72	20.6	4.08	26.0	2.74	2.20	2.58	2.84	2.57	6.16
6	2.40	2.14	2.00	2.32	15.4	3.69	4.54	20.3	6.02	25.9	4.26	3.14	2.75	2.44	1.90	6.61

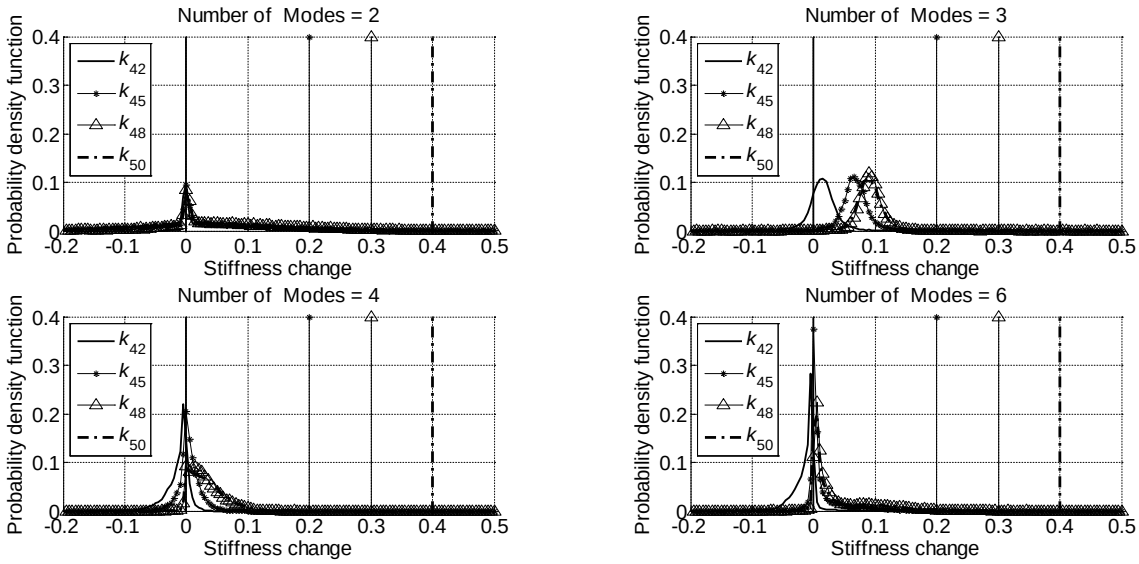

Figure 5. Histogram of selected parameters by modal property difference approach

substructure model. An iterative linearization procedure is adopted for efficiently solving the model updating problem.

The presented substructure updating approach is validated on a 200-DOF spring mass model. For comparison, a conventional modal property difference approach is also studied. In the noise-free case, the error from the modal dynamic residual approach and the modal property difference approach is close to zero. Monte Carlo simulation is then conducted to generate experimental modal properties contaminated with noise, and the updating results from the modal dynamic residual approach are overall better than those from the modal property difference approach. In the future, further analytical and numerical studies are needed on the convergence, accuracy, and computational efficiency of the modal dynamic residual approach for substructure model updating under noisy measurements.

5. Acknowledgement

This research is partially sponsored by the National Science Foundation (#CMMI-1150700 and #CMMI-1041607), the Research and Innovative Technology Administration of US DOT (#DTRT12GUTC12), and Georgia DOT (#RP12-21). Any opinions, findings, and conclusions or recommendations expressed in this publication are those of the authors and do not necessarily reflect the view of the sponsors.

REFERENCES

Ahmadian, Mottershead & Friswell. "Regularisation methods for finite element model updating". *Mechanical Systems and Signal Processing*, 1998; 12(1), 47-64.

Alvin. "Finite element model update via Bayesian estimation and minimization of dynamic residuals". *AIAA Journal*, 1997; 35(5), 879-886.

Collins, Hart, Haselman & Kennedy. "Statistical identification of structures". *AIAA Journal*, 1974; 12(2), 185-190.

Craig & Bampton. "Coupling of substructures of dynamics analyses". *AIAA Journal*, 1968; 6(7), 1313-1319.

Farhat & Hemez. "Updating finite element dynamic models using an element-by-element sensitivity methodology". *AIAA Journal*, 1993; 31(9), 1702-1711.

Friswell & Mottershead. *Finite element model updating in structural dynamics*. Dordrecht; Boston: Kluwer Academic Publishers, 1995.

Hoshiya & Saito. "Structural identification by extended kalman filter". *Journal of Engineering Mechanics*, 1984; 110(12), 1757-1770.

Jaishi & Ren. "Damage detection by finite element model updating using modal flexibility residual". *Journal of Sound and Vibration*, 2006; 290(1-2), 369-387.

Jaishi & Ren. "Structural finite element model updating using ambient vibration test results". *Journal of Structural Engineering*, 2005; 131(4), 617-628.

Koh, See & Balendra. "Estimation of structural parameters in time domain - a substructure approach". *Earthquake Engineering & Structural Dynamics*, 1991; 20(8), 787-801.

Link. "Updating analytical models by using local and global parameters and relaxed optimisation requirements". *Mechanical Systems and Signal Processing*, 1998; 12(1), 7-22.

Mathworks Inc. *Control System Toolbox : for Uses with MATLAB® : Getting Started* (Version 6. ed.). Natick, MA: MathWorks Inc., 2005.

Park, Park, Ahn & Lee. "1-Norm-based regularization scheme for system identification of structures with discontinuous system parameters". *International Journal for Numerical Methods in Engineering*, 2007; 69(3), 504-523.

Sipple & Sanayei. "Finite element model updating using frequency response functions and numerical sensitivities". *Structural Control and Health Monitoring*, 2014; 21(5), 784-802.

Zhang & Johnson. "Substructure identification for shear structures II: Controlled substructure identification". *Structural Control and Health Monitoring*, 2013; 20(5), 821-834.

Zhu, Dong & Wang. "Substructure model updating through iterative minimization of modal dynamic residual".*Proceedings of SPIE, Nondestructive Characterization for Composite Materials, Aerospace Engineering, Civil Infrastructure, and Homeland Security*, 2014, San Diego, California, USA.